REPORT DOCUMENTATION PAGE

Form Approved
OMB No. 0704-0188

1. REPORT DATE *(DD-MM-YYYY)*	**2. REPORT TYPE**	**3. DATES COVERED** *(From - To)*
18 June 2015	Book Chapter	March 2015 – June 2015

4. TITLE AND SUBTITLE
Structure-Property Relationships for Polycyanurate Networks Derived from Renewable Resources

5a. CONTRACT NUMBER

5b. GRANT NUMBER

5c. PROGRAM ELEMENT NUMBER

6. AUTHOR(S)
Andrew J. Guenthner; Benjamin G. Harvey; Matthew C. Davis; Michael D. Ford; Heather A. Meylemans; Michael E. Wright; Andrew P. Chafin; Joseph M. Mabry

5d. PROJECT NUMBER

5e. TASK NUMBER

5f. WORK UNIT NUMBER
Q0BG

7. PERFORMING ORGANIZATION NAME(S) AND ADDRESS(ES)

Air Force Research Laboratory (AFMC)
AFRL/RQRP
10 E. Saturn Blvd.
Edwards AFB, CA 93524-7680

8. PERFORMING ORGANIZATION REPORT NO.

9. SPONSORING / MONITORING AGENCY NAME(S) AND ADDRESS(ES)

Air Force Research Laboratory (AFMC)
AFRL/RQR
5 Pollux Drive
Edwards AFB, CA 93524-7048

10. SPONSOR/MONITOR'S ACRONYM(S)

11. SPONSOR/MONITOR'S REPORT NUMBER(S)
AFRL-RQ-ED-BK-2015-087

12. DISTRIBUTION / AVAILABILITY STATEMENT
Approved for public release; distribution unlimited

13. SUPPLEMENTARY NOTES
For publication in American Chemical Society (18 June 2015); Chapter 26, pp 431–452
PA Case Number: #15124; Clearance Date: #3/15/2015

14. ABSTRACT
The recent synthesis of a wide variety of cyanate ester monomers that may be derived from renewable resources has created a newly available set of chemical structures that, due to a wide range of chemical features, provide a unique opportunity for the development of quantitative structure-property relationships for dicyanate esters and their polymerized networks. Specific structure-property relationships for monomer melting point, glass transition temperature at full conversion, and char yields at 600 °C under nitrogen and air have been developed with the aid of partial least squares methods. The predictions inherent in these structure-property relationships are examined and compared to predictions based on ordinary least squares methods. Specific predictions for the properties of two as-yet unsynthesized dicyanate ester monomers derived from renewable resources are also presented.

15. SUBJECT TERMS
N/A

16. SECURITY CLASSIFICATION OF:			**17. LIMITATION OF ABSTRACT**	**18. NUMBER OF PAGES**	**19a. NAME OF RESPONSIBLE PERSON**
					J. Mabry
a. REPORT	**b. ABSTRACT**	**c. THIS PAGE**	SAR	23	**19b. TELEPHONE NO** *(include area code)*
Unclassified	**Unclassified**	**Unclassified**			N/A

Standard Form 298 (Rev. 8-98)
Prescribed by ANSI Std. 239.18

RESERVE THIS SPACE

Structure-Property Relationships for Polycyanurate Networks Derived from Renewable Resources

Andrew J. Guenthner*[1], Benjamin G. Harvey[2], Matthew C. Davis[2], Michael D. Ford[3], Heather A. Meylemans[2], Michael E. Wright[2], Andrew P. Chafin[2], and Joseph M. Mabry[1]

[1]Air Force Research Laboratory, Aerospace Systems Directorate, 10 E. Saturn Blvd. Edwards AFB,CA 93524, USA
***E-mail: andrew.guenthner@us.af.mil**
[2]Naval Air Warfare Center, Weapons Division, 1 Administration Circle, China Lake, CA 93555, USA
[3]ERC Incorporated, Air Force Research Laboratory, 10 E. Saturn Blvd, Edwards AFB, CA 93524, USA

The recent synthesis of a wide variety of cyanate ester monomers that may be derived from renewable resources has created a newly available set of chemical structures that, due to a wide range of chemical features, provide a unique opportunity for the development of quantitative structure-property relationships for dicyanate esters and their polymerized networks. Specific structure-property relationships for monomer melting point, glass transition temperature at full conversion, and char yields at 600 °C under nitrogen and air have been developed with the aid of partial

RESERVE THIS SPACE

least squares methods. The predictions inherent in these structure-property relationships are examined and compared to predictions based on ordinary least squares methods. Specific predictions for the properties of two as-yet unsynthesized dicyanate ester monomers derived from renewable resources are also presented.

Introduction

Polycyanurate networks, which are produced by cyclotrimerization of cyanate ester monomers, are a well-known class of high-performance thermosetting polymers that offer many unique advantages in demanding applications.[1-4] For instance, in structures for space telescopes[5] and interplanetary space probes,[6] the ease of polymerization with little or no generation of volatiles is especially advantageous for reliable long-term performance. Similarly, the unusually low dielectric constants, outstanding resistance to high-energy radiation, and low coefficients of thermal expansion of polycyanurate networks provide additional advantages in the harsh environments of outer space or on other planets. In terrestrial environments, the high mechanical strength and stiffness of polycyanurate networks at elevated temperatures are attractive for applications in micro-electronics and aircraft engines.[7] From a fundamental standpoint, polycyanurates are advantageous for the study of structure-property relationships in thermosetting networks because the high selectivity of cyanurate formation results in networks with chemical structures that can be described with much greater precision than is possible with many other networks.[8] The ease of network preparation, relatively low toxicity of monomers, and the ability to adjust reaction rates over a wide range through catalysis also greatly aid in carrying out studies of the relationship between network structure and properties.

At first glance, it may appear that polycyanurate networks are not an especially appealing class of polymers for replacement of petroleum-based sources with bio-based or other renewable sources, because traditionally, bio-based sources have been desired for their relatively low cost, with the expectation that significant declines in performance will be a necessary trade-off. Such reasoning, however, fails to take into account considerations of source variety. Cyanate ester monomers derived from petroleum sources have tended to fall into two distinct classes: bisphenol-type monomers that are derived from the coupling of phenol with ketones, or novolac-type monomers that are derived from the coupling of phenol and formaldehye.[1] Because of its wide availability as a standard petroleum product, the use of phenol as a starting point for monomer synthesis has become an entrenched practice. In the realm of

renewable sources, however, there is no bias toward phenol as a starting point. The plant kingdom offers a wide variety of phenolic compounds that may be obtained from essential oils, extracts, or from the decomposition of lignin.

From the perspective of performance, a wider variety of starting structures will enable the synthesis of networks with a wider variety of final properties. While some property combinations may offer lower performance, others will offer higher performance. For example, polycyanurate networks derived from the essential oil anethole have been shown to offer the lowest known water uptake near full conversion (1.1%) in networks that exhibit a glass transition temperature above 220 °C at full conversion and that can be produced from monomers that are stable liquids at room temperature.[9] This combination of properties is particularly useful for production of structures by bulk molding for use in environments with both exposure to moisture and elevated temperature

From the perspective of developing structure-property relationships, the wide variety of structures afforded by renewable resources that can be converted into monomers is extremely useful. In most cases, the ultimate goal driving the development of structure-property relationships is the desire to rationally design a network at the molecular level to satisfy a given set of performance needs, based on the predicted properties of structures that have not yet been synthesized. The usefulness of such predictions depends on their reliability for structures that differ from those already available. The reliability in turn depends on the variety of available structures utilized to elucidate the structure-property relationships that enable prediction. The availability of a greater variety of structures from renewable resources will therefore translate into more robust structure-property relationships that can be used to generate more reliable predictions of performance. Thus, the development of polycyanurate networks based on renewable resources has afforded a unique opportunity to study structure-property relationships in a class of thermosetting polymers where both the structures are known with a high level of precision and a wide range of structures have been characterized.

In this chapter, the structure-property relationships in polycyanurate networks derived from renewable resources will be discussed with respect to four key properties: monomer melting point, glass transition temperature at full conversion, and char yields under nitrogen and air at 600 °C. These properties were chosen because they generally do not depend on the extent of conversion in the network. The first two are independent of conversion by definition, and the latter two, while they may show some conversion dependence, are the outcome of experiments in which the networks are heated to very high temperatures, thereby likely resulting in very high levels of conversion at the onset of degradation. The structure-property relationships, which are derived from partial least squares (PLS) regressions on the properties of interest as a function of quantitative structural parameters, are compared to more traditional linear regression analysis. We found the PLS technique to be effective in

elucidating known structure-property relationships, even with a data set typically consisting of only around 15 samples. The majority of these relationships are known only because of the availability of bio-based monomers.

Experimental

Materials and Data Sources

The 19 monomers / networks chosen for analysis contain only the elements C, H, N, and O. All feature two aromatic rings containing one or more cyanate ester / cyanurate linkages, connected by a bridge containing only non-aromatic hydrocarbons. Two of the monomers are derived from petroleum; they are the well-known Primaset BADCy and Primaset LECy (dicyanate esters of bisphenol A and E, respectively); the remaining 17 have been derived from a variety of plant compounds. Figure 1 shows the chemical structure of all monomers, along with the nomenclature used to identify them. The networks chosen for comparison have all been analyzed using either identical or nearly identical protocols in our laboratories, thereby helping to ensure that comparisons reflect meaningful differences. Table 1 lists the properties of interest for all of these materials, along with the original source publications,[9-15] where available. In some cases, as noted in the table, publication is in progress.

Methods of Analysis

An advantage of PLS regression is that there is no need to try and guess which structural parameters are of importance ahead of time, nor is there a need to try and combine parameters judiciously so as to produce mechanistically relevant independent variables or to limit correlations in the structural parameters. Instead, all that is necessary is to produce a consistent scheme of non-duplicative parameters that are capable of describing the structure. It might be assumed that because of the highly similar nature of the monomers, that the number of structural parameters would be small. However, as Figure 2 shows, we found that a minimum of ten parameters was necessary to describe these systems. Five parameters describe the ~~subsituttion~~ substitution patterns around the aromatic rings, which are usually but not always the same for both rings in each monomer. The other five describe the architecture of the bridge. Six of the parameters take on values from 0 to 1, while four (all associated with the bridge) can take on any number larger than 0. Table 2 provides extended definitions for each parameter, while Figure 2 provides a convenient graphical way to visualize

the meaning of each parameter. We could have included additional parameters, however, we chose not to include parameters which were unique to a single monomer because these parameters simply become correction factors that are unique to that particular monomer. Thus, for instance, with regard to methyl

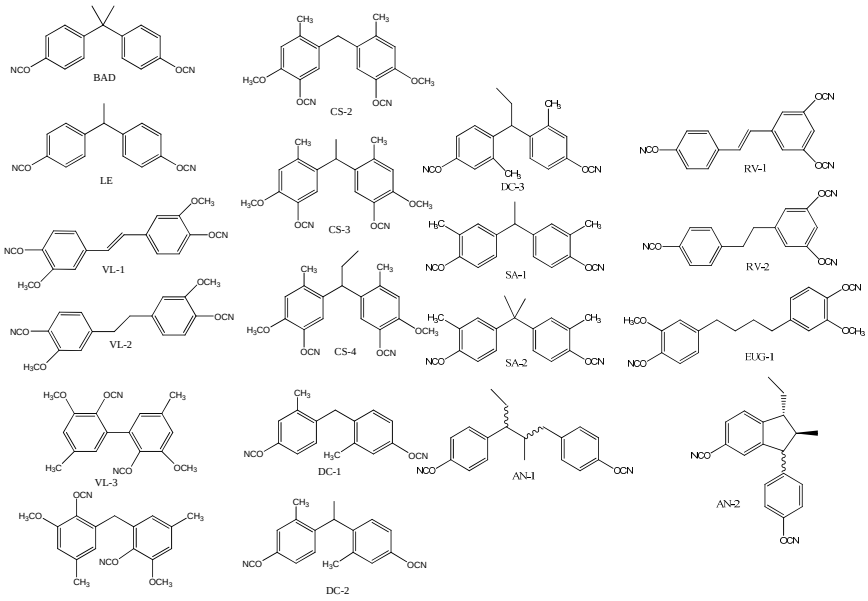

Figure 1. Structures of monomers included in correlations, with labels.

groups on aromatic rings, we do distinguish between *–ortho* substitution and other substitution patterns, but not between *–meta* and *–para* substitution.

For monomers containing different structures on each ring, the values were averaged. For instance, in resveratrol, one but not both rings have an additional –OCN group, therefore the "additional –OCN" parameter has a value of 0.5, just as the "kinked chain" parameter also takes on a value of 0.5. Note that for the bridge groups, in accordance with a method described by Bicerano,[16] we assume that aliphatic rings have intermediate flexibility between that of aromatic rings and linear aliphatics, with fused rings biased toward increased rigidity. For AN-2, this required that the bridge atoms be partitioned among the various parameters. For the single atom in the backbone, we apportioned 0.5 to the flexible backbone parameter FB and the remaining 0.5 to the rigid backbone parameter. Similarly, for the side groups, taking into account that only one atom clearly meets the definition of "flexible,~~:~~", we partitioned 1.5 atoms to the flexible side group parameter and 3.5 to the rigid side group parameter, which includes terminal methyl group carbons. Table 3 lists the values of these

parameters for all of the monomers / networks studied. It is worth noting that, like all structural parameterizations, the one developed for this study has limitations. CS-1 and CS-2, for instance, have exactly the same structural parameters, despite differing in the type of "kink" found in the chain. This

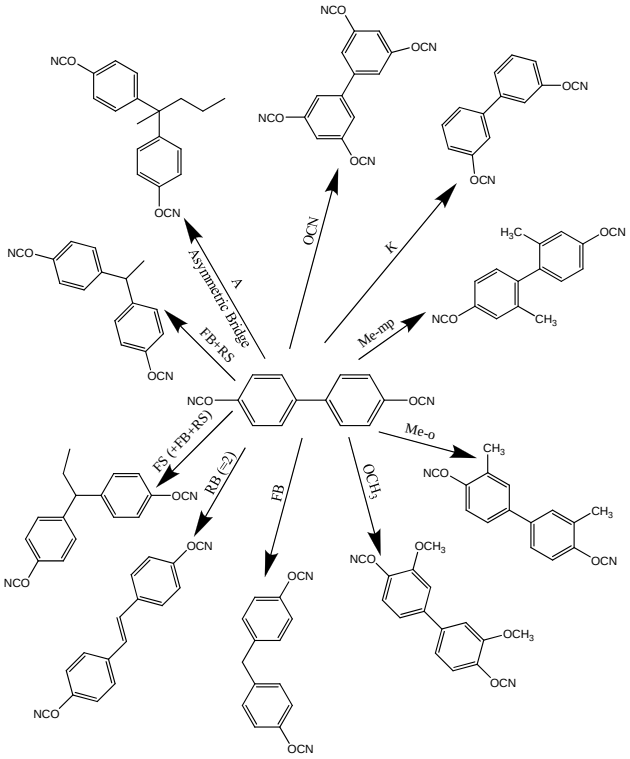

Figure 2. Illustration of the structural parameters used in developing structure-property correlations. The "baseline monomer" structure is shown in the center, with the arrows describing the unit changes to parameters that result in the modified structures shown on the outer circle. For instance, changing the parameter K from 0 to 1 results in the structure shown in the upper right corner. Note that in some case, sensible structures result only from multiple simultaneous changes if starting with the "baseline" monomer.

limitation stems from the decision not to include structural parameters that were unique to a single monomer.

For each property of interest, a partial least squares regression was done on all samples with measured data (typically 14 to 17 of the 19 available monomers). The PLS regressions were carried out using the SIMPLS algorithm[17] in MATLAB. This algorithm automatically centers the input data

but does not require normalization. The regressions were repeated while varying the number of PLS components from 0 to 9, and, in each case, the mean squared error of the regression was estimated using "leave one out" cross-validation. The number of PLS components was then chosen so as to minimize the estimated mean squared error, and detailed information was gathered on the selected regression. More traditional linear regressions were also carried out, first using all structural parameters, and then using only those parameters that were found to be significant in some cases The latter approach represents a more traditional means of reducing the effects of overfitting, which would likely be attempted if PLS were not available.

Table 1. Physical property data used in structure-property correlations

Monomer/network	T_m (°C)[a]	$T_{G\text{-}fc}$ (°C)[b]	Char Yield (N_2, %)	Char Yield (Air, %)	Source
BAD	83	323	47	25	9
LE	Liquid[c]	295	54	24	9
AN-1	Liquid[c]	223	31	9	9
AN-2	72	313	48	6	9
CS-1	151	236	33	8	10
CS-2	125	240	35	11	10
CS-3	98	206	28	11	10
CS-4	120	238	27	11	10
DC-1	88	259	53	30	11[d]
DC-2	105	283	43	4	11[d]
DC-3	Liquid[c]	273	43	3	11[d]
EUG-1	104	167	31	1	12
RV-1	156	>340	74	71	13
RV-2	123	334	70	66	13
SA-1	73	236	48	11	14
SA-2	82	237	43	8	14
VL-1	237	n/a	n/a	n/a	15
VL-2	190	n/a	n/a	n/a	15
VL-3	205	n/a	n/a	n/a	15

a. Melting point as observed by differential scanning calorimetry b. Glass transition temperature as determined by peak in loss component of stiffness in oscillatory thermomechanical analysis after heating to 350 °C c. No differential scanning calorimetry melting point was observed d. Publication in progress. Numbers in the "source" column refer to the number of the reference given at the end of this chapter in which the data are located.

Table 2. Explanation of structural parameters

Parameter	Explanation
OCN	Additional -OCN groups per monomer (e.g. 1 for tricyanates)
K	"Kinked" -OCN groups (that is, -OCN groups -*ortho* or -*meta* to bridge junction); 1 if any such groups are present on a cyanated aromatic ring; 0 if not present on a cyanated ring; averaged over all cyanated aromatic rings in monomer (e.g. 0 for the typical 4,4' –OCN substitution pattern in dicyanate monomers)
Me-mp	Methyl groups in positions -*meta* or -*para* to -OCN groups; 1 if any such groups are present on a single aromatic ring; 0 if not present; averaged over all cyanated aromatic rings in monomer
Me-o	Methyl groups in positions -*ortho* to -OCN groups; counting / averaging rules are the same as for Me-mp.
OCH_3	Methoxy groups on cyanated aromatic rings; counting / averaging rules are the same as for Me-mp
FB	"Flexible" non-hydrogen atoms in bridge "backbone" structure; the "backbone" of the bridge is defined as the set of non-hydrogen atoms bonded along the shortest possible path connecting two cyanated aromatic rings; if more than one such path exists, atoms in all such paths count, if more than one bridge exists, the total number of flexible non-hydrogen atoms in all bridge structures is counted, with each counted only once; "flexible" is defined as having sp^3 hybridization and being bonded to at least two other atoms (e.g. not a chain terminus) not in a ring; sp^3 atoms in ring structures considered on a case by case basis.
RB	"Rigid" non-hydrogen atoms in bridge "backbone" structure. "Rigid" is defined as any non-hydrogen atom not meeting the criteria for "flexible", with sp^3 atoms in ring structures considered on a case by case basis. Non-hydrogen atoms that terminate chains, such as methyl carbons, and hydroxyl oxygens, count as "rigid". Rules for backbones and bridges are the same as for FB.
FS	"Flexible" non-hydrogen atoms in bridge "side group" structures. "Flexible" is defined as in FB, and the rules for counting paths and bridges are the same as in FB. A "side group" atom is any non-hydrogen atom in a structure bridging cyanated aromatic rings that is not counted as part of the "backbone"
RS	"Rigid" non-hydrogen atoms in "side group" bridge structures; definitions and rules are the same as for FB, RB, and FS (e.g. an isopropylidene bridge will have FB=1 and RS=2).
A	Asymmetric bridge. 1 if a bridge group is symmetrically substituted along its backbone(s), 0 if not, averaged over all bridge structures. Bridge and backbone are defined as in FB.

Table 3. Structural parameter values for all monomers

Monomer	OCN	K	Me-mp	Me-o	OCH3	FB	RB	FS	RS	A
BAD	0	0	0	0	0	1	0	0	2	0
LE	0	0	0	0	0	1	0	0	1	1
AN-1	0	0	0	0	0	3	0	1	2	1
AN-2	0	0	0	0	0	0.5	0.5	1.5	3.5	1
CS-1	0	1	1	0	1	1	0	0	0	0
CS-2	0	1	1	0	1	1	0	0	0	0
CS-3	0	1	1	0	1	1	0	0	1	1
CS-4	0	1	1	0	1	1	0	1	1	1
DC-1	0	0	1	0	0	1	0	0	0	0
DC-2	0	0	1	0	0	1	0	0	1	1
DC-3	0	0	1	0	0	1	0	1	1	1
EUG-1	0	0	0	0	1	4	0	0	0	0
RV-1	1	0.5	0	0	0	0	2	0	0	0
RV-2	1	0.5	0	0	0	2	0	0	0	0
SA-1	0	0	0	1	0	1	0	0	1	1
SA-2	0	0	0	1	0	1	0	0	2	0
VL-1	0	0	0	0	1	0	2	0	0	0
VL-2	0	0	0	0	1	2	0	0	0	0
VL-3	0	1	1	0	1	0	0	0	0	0
AN-U	0	0	0	0	0	1	2	1	2	1
EUG-U	0	0	0	0	1	2	0	0	0	0

Results and Discussion

Monomer Melting Point

Of the 19 monomers studied, melting points were measured for 16. The remaining three had melting points that were near or below room temperature, making measurement difficult. In the case of LECy, the melting point is known to be 29 °C, a value likely depressed significantly due to the presence of two co-crystalline forms,[18] however, we did not include this melting point in the data set for reasons of consistency. It is not known whether the other "liquid" cyanate ester monomers are also simply supercooled liquids with melting points near room temperature, so only those melting points that were observed in a standard

DSC experiment were included. In general, we have found that melting points of cyanate esters vary widely and do not conform to simple structural rules, therefore a model based on PLS regression may be quite useful. In this section, the melting point model is examined in some detail in order to illustrate the concepts underlying all of the PLS models described in this chapter.

Figure 3 shows that with just three components, PLS regression provides the minimum error according to cross-validation. In contrast, the root-mean-squared ("rms") error of the regression itself continues to decrease as more components are added. Note that the use of 10 components yields a model equivalent to ordinary least squares regression. The three component model explains about 83% of the variation in melting point. Although the 10-component model can explain 95% of the variation, this comes at the cost of over-prediction, as expected for a data set with just 16 samples.

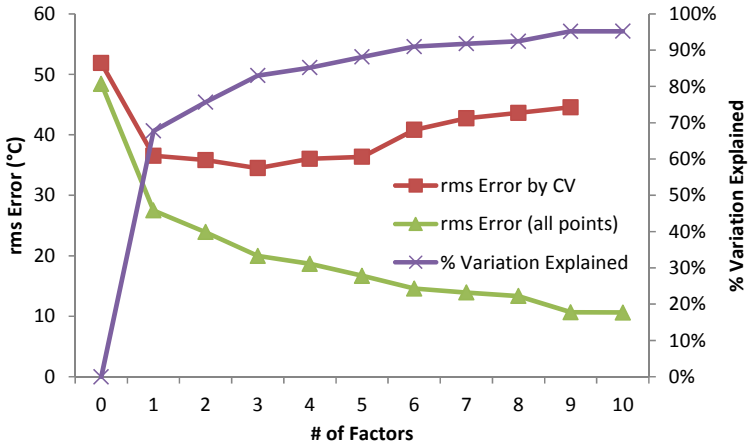

Figure 3. Partial least squares regression characteristics as a function of the number of regression components present.

In order to understand how over-prediction affects the data set, Figure 4 shows the predicted melting points for each of the samples as a function of the number of PLS components added. The PLS regression process can be thought of generating a set of successively corrected predictions for the observed results. As Figure 4 shows, the first two or three components (which can be considered iterations in successive prediction) affect nearly all of the predictions, whereas later iterations affect only a few. Note that the shaded area in Figure 4 indicates where over-prediction takes place according to cross-validation experiments. In more colorful terms, the first three components can be thought of as "catering to the masses," whereas the additional components can be envisioned as "catering to special interests."

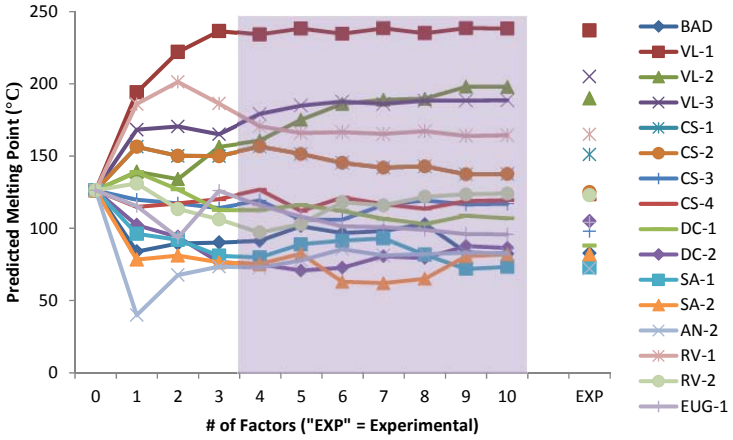

Figure 4. Predicted melting point values as a function of the number of partial least squares regression components.

The effect of "catering to special interests" on the quantitative model for monomer melting point can be seen in Figure 5. The values plotted reflect the relative effect of a unit change in each of the structural parameters on the predicted melting point. Note that "const." refers to the model intercept. With few components, the model generally features a cluster of features that tend to depress the melting point, with the presence of flexible backbone linkages in the bridge and rigid or terminal side groups on the bridge having the largest relative effects. In contrast, the presence of rigid backbone linkages and methoxy groups *ortho*- to the cyante ester groups tend to result in a significant increase in melting point. However, as more components are added, many of the coefficients "blow up". For instance, the predicted effect of methoxy groups triples in magnitude, while the effect of having one additional –OCN linkage per aromatic ring is transformed from insignificant to an almost 150 °C increase, and the effect of "kinked" –OCN groups is transformed from insignificant to an over 100 °C decrease. In fact, Figure 5 makes clear that the most significant effects indicated by ordinary linear regression are actually just those effects that have been "blown up" the most by over-prediction.

For prediction of melting points, then, it can be seen that ordinary least squares leads to over-prediction, in which "catering to special interests" by the model (that is, reducing the errors in predicting the values of a few select data points) leads to estimates of structural effects that are wildy different than those found in models that reduce prediction errors across the entire sample set. These results demonstrate that the typical advantages of PLS regression are realized when constructing structure-property models on relatively small data sets.

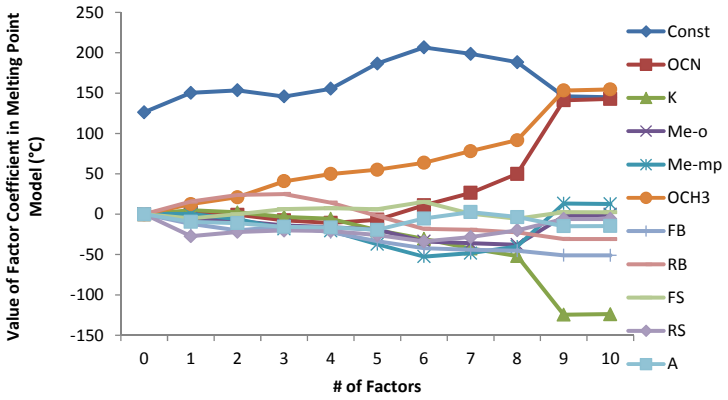

Figure 5. Melting point regression coefficients as a function of the number of partial least squares regression components.

Having established the model, it is important to consider the actual predictive capabilities it provides. Cross-validation indicates that the PLS regression should predict melting points to within about 35 °C. As a result, for samples (such as LECy) not included in the model, the predicted melting points should be not much greater than about 50 °C. Figure 6 shows the predicted melting points (Table 4 provides the model coefficients) according to both ordinary least squares (OLS) and PLS regressions for LECy, DC-3, and AN-1, the three "room temperature liquid" monomers. Both models predict that only AN-1 should be liquid at room temperature. As mentioned earlier, the melting points of monomers such as LECy appear to be anomalously low due to the ease of producing disorder in the crystalline structure. Other studies of cyanate esters have shown the monomers may be liquid at room temperature due to the presence of multiple stereoisomers,[19] as would be the case for AN-1. Thus, although the models may be able to quantify the expected value of the melting point, many complex physical and chemical factors will also play a role.

In Figure 6, the predicted melting points according to OLS and PLS regressions for two as-yet unsynthesized monomers are given. These are the unsaturated forms of the AN-1 and EUG-1 monomers. The synthesis of both monomers involves a hydrogenation step that may be skipped in order to produce the structures AN-U and EUG-U (shown in Figure 7). As of this writing, these monomers have not been made, thus the predicted melting points shown in Figure 6 cannot have been influenced by any experimental findings to date. The OLS model predicts that AN-U should be a liquid like AN-1, while the PLS model predicts that AN-U will be a solid with a melting point in the 100-150 °C range. These contrasting predictions will provide an interesting test of these models should the compound AN-U be synthesized.

Table 4. Linear regression model coefficients for melting point

Factor	PLS	OLS
Constant	145.88	144.97
OCN	-7.64	142.86
K	-3.44	-123.97
Me-o	-13.73	-0.42
Me-mp	-18.07	12.73
OCH3	40.74	154.55
FB	-15.17	-50.97
RB	24.92	-30.87
FS	6.21	2.37
RS	-20.27	-5.86
A	-15.69	-14.60

Regression types: PLS = partial least squares; OLS = ordinary least squares

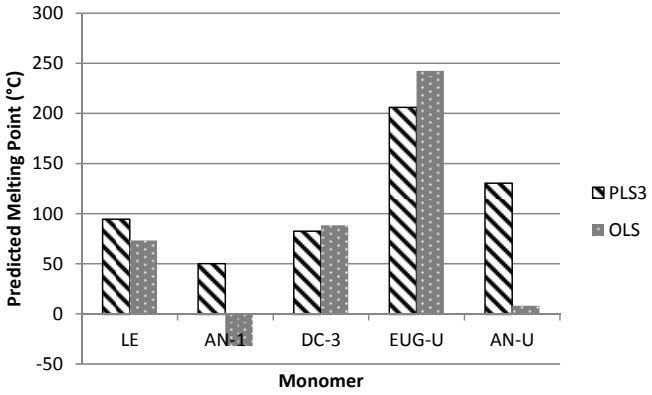

Figure 6. Predicted melting points of monomers not included in regression models; comparison of ordinary least squares and partial least squares predictions.

Glass Transition Temperature at Full Cure

Figure 8 shows the error characteristics of the PLS model of the glass transition temperature at full cure. In this case, 15 of the 19 samples were used for the model. RV-1 was excluded because its glass transition temperature at full cure was too high to be measured reliably, while degradation of the

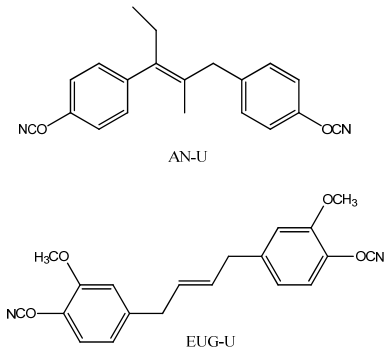

Figure 7. Chemical structures of the as-yet unsynthesized monomers AN-U and EUG-U.

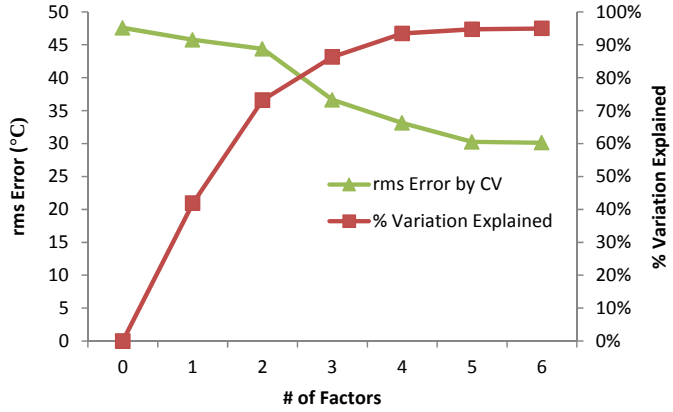

Figure 8. Error characteristics of partial least squares model for glass transition temperature at full cure.

networks interfered with the measurement of the glass transition temperature at full cure for the systems with monomers derived from vanillin. With six components, the rms error based on cross-validation is minimized, and over 95% of the variation is accounted for. Similar to the regression for melting point, the minimum rms error is around 30 °C.

Figure 9 shows the predicted glass transition temperature values as a function of the number of PLS components. Unlike the case with melting point, as more components are added, the adjustments become finer but remain spread out more or less evenly over at least five different samples. This result indicates that the PLS regression algorithm is still "catering to the masses" as errors are reduced, rather than "catering to special interests."

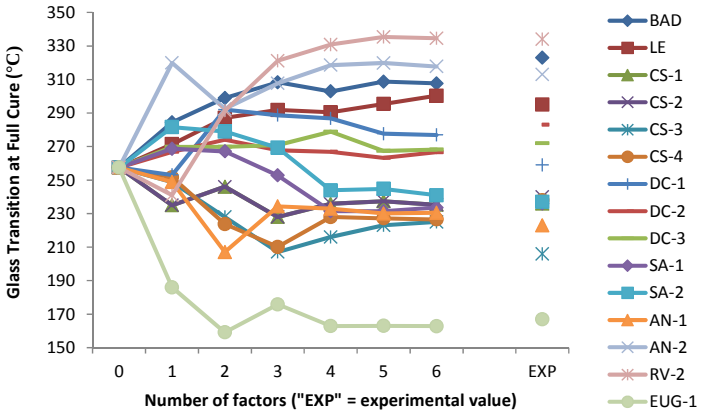

Figure 9. Predicted glass transition temperature values as a function of the number of partial least squares components utilized in the model.

In order to examine the predictive capabilities of the models, the glass transition temperature at full cure was predicted for RV-1, and the as-yet unsynthesized monomers AN-U and EUG-U. The PLS regression was compared to ordinary least squares (OLS), and ordinary least squares in which only statistically significant factors were retained (OLS-r). The OLS-r model represents an alternative means of avoiding the pitfalls of over-prediction. For RV-1, which is known to have a glass transition temperature at full cure significantly exceeding 340 °C (not to be confused with the "as cured" glass transition temperature, which is lower due to incomplete conversion), the PLS model predicts a glass transition temperature near 410 °C, while the OLS and OLS-r models predict much lower values of 280 °C and 300 °C, respectively. Table 5 lists the coefficients and Figure 10 shows the predicted values. In contrast, for the closely related RV-2, both PLS and OLS predict a glass transition temperature near 350 °C, which agrees well with the experimental value of 334 °C, while the OLS-r model predicts a much lower glass transition temperature of 250 °C. The PLS model thus does a good job of "extrapolating" the model to predict the properties of a structure that is not included in the model but is closely related, while the OLS model "extrapolates" poorly, predicting that the more rigid RV-1 will have a significantly lower glass transition temperature compared to RV-2, in contrast to both conventional heuristics and the available qualitative observations.

Both OLS models therefore contradict known experimental data. The PLS model shows that increased cyanate ester density increases the glass transition temperature, as does the OLS model. All three models show that adding a

methyl group –*ortho* to the cyanate ester decreases the glass transition by about 35 °C compared to the addition of a methyl group either –*met*a or –*para* to the cyanate ester, an observation noted earlier by us.[15] All models also agree that adding flexible linkages in the bridge lowers the glass transition temperature, a prediction that is in general agreement with observed glass transition temperature trends in polymers. The PLS model indicates that the addition of methoxy groups to the aromatic rings decreases the glass transition temperature, a sensible result given the known effects of methyl group subsitution.

For AN-U and EUG-U, both PLS and OLS-r models predict higher glass transition temperature values, of 250 – 300 °C at full cure, compared to the OLS model, which predicts values of 170 °C and 110 °C, respectively, for AN-U and EUG-U. Significantly, the OLS model predicts that the glass transition temperatures of AN-U and EUG-U will be substantially lower than those of the more flexible, hydrogenated analogues. These predictions seem highly counter-intuitive, and are likely the result of the "RB" coefficient experiencing a "blow up" due to over-prediction in the OLS model.

Char Yields in Nitrogen and Air

Char yield data was available on 16 out of the 19 networks (all but the vanillin-based systems). The char yields measured were at 600 °C after heating at 10 °C/min. in both nitrogen and air. Generally, the thermal degradation behavior of cyanate esters in nitrogen and air is quite similar. However, additional degradation in air often begins at temperatures just under 600 °C. As a result, the char yields in air can be quite sensitive to the onset of this secondary degradation, which in turn is sensitive to the details of the primary degradation process. As a result, it can be difficult to correlate char yields in air to specific structural features.

For the char yields in nitrogen, a two-component PLS model minimized the prediction error according to cross-validation experiments, while for char yields in air, seven components were required. In general, the prediction errors were larger for char yields in air, likely due to the greater sensitivity of this variable to the specific details of the decomposition process, as explained earlier. Figure 11 shows the characteristic errors obtained by cross-validation as well as the amount of variation explained by PLS models for char yields in nitrogen and in air as a function of the number of PLS components.

Figures 12 and 13 show the predicted char yield values as a function of the number of PLS components for both nitrogen and air, respectively. Note how, although major changes take place in the first few components, they are distributed among several samples rather than just one or two. Note also how, in Figure 13, the subtle changes in the predictions caused by addition of the sixth

Table 5. Linear regression model coefficients for glass transition temperature at full cure.

Factor	PLS	OLS	OLS-r
Constant	345.45	355.59	297.61
OCN	58.52	90.519	0
K	1.13	-38.66	0
Me-o	-66.72	-72.50	-35.17
Me-mp	-33.56	-36.40	0
OCH3	-42.84	-3.04	0
FB	-34.95	-46.39	-25.94
RB	2.48	-73.01	0
FS	1.53	10.50	0
RS	-1.41	3.52	0
A	-8.81	-10.98	0

Regression types: PLS = partial least squares; OLS = ordinary least squares; OLS-r = ordinary least squares re-calculated with only signficiant factors included

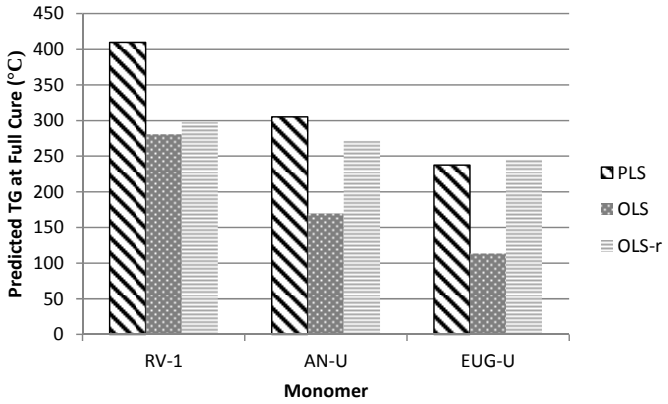

Figure 10. Predicted glass transition temperature values for networks not included in models; comparison of predictions by model type.

and seventh factors do not appear to be significant, however, when vieweing the rms error according to cross-validation shown in Figure 11, the addition of these factors does result in a 20% reduction in prediction error by cross-validation. This apparent difference is an indication that the predictive model for char yields in air may be sensitive to the exclusion of a single data point.

The predictive capabilities of the models are illustrated in Figure 14. (Table 6 provides model coefficients). Although char yields at 600 °C were not available for VL-1 and VL-2, some TGA experiments have been done. These

show ~80% and ~60% char yields at about 400 °C under nitrogen after accounting for the loss of trapped solvent, values which are roughly consistent with the predicted char yields at 600 °C. The predicted char yields of AN-U and EUG-U are also shown. In general, the model coefficients indicate that aromatic substitution patterns and the density of cyanate ester linkages are key factors controlling char yields, with methoxy group substitution having a particularly negative effect. The negative effect of methoxy group substitution on thermo-chemical stability in general has been noted in studies of cyanate esters.

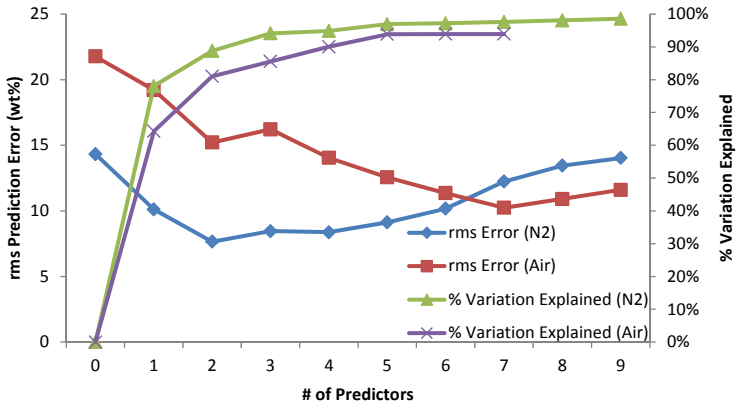

Figure 11. Error characteristics of partial least squares regressions for char yield.

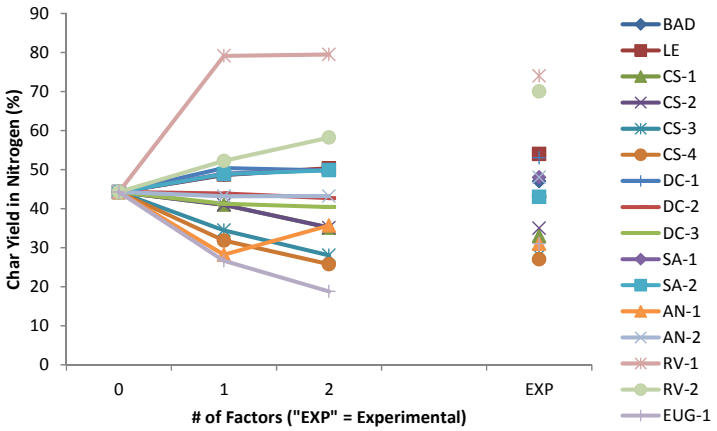

Figure 12. Predicted char yield values as a function of the number of partial least squares regression components, for char yields in nitrogen.

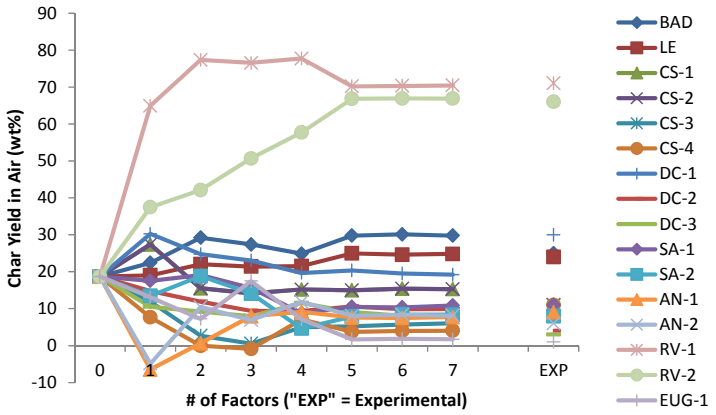

Figure 13. Predicted char yield values as a function of the number of partial least squares regression components, for char yields in air.

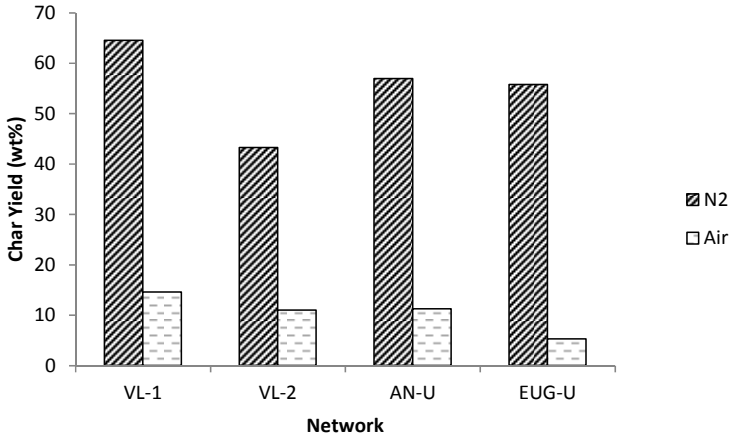

Figure 14. Predicted char yields of networks not included in models.

Table 6. PLS linear regression model coefficients for char yield.

Factor	Char Yield (N_2, %)	Char Yield (Air, %)
Constant	61.77	38.73
OCN	7.62	30.20
K	-4.88	14.49
Me-o	-0.38	-13.97
Me-mp	-7.62	-14.87
OCH3	-9.77	-18.42
FB	-4.38	-4.65
RB	6.26	-2.87
FS	-2.30	-1.95
RS	-3.59	-5.86
A	-3.50	-3.40

Conclusions

Using a set of 19 cyanate ester monomers, 17 of which may be derived from renewable sources, structure property relationships, in the form of partial linear regression models, have been produced for the monomer melting point, glass transition temperature at full cure, and char yield at 600 °C under nitrogen and in air. The partial least squares method was able to provide linear models based on a set of 10 structural parameters that predicted melting points to within about 35 °C, glass transition temperatures at full cure to within about 30 °C, and char yields to within about 10%, based on "leave one out" cross-validation analysis. The predictive power of the patial least squares models was compared to that of ordinary least squares and shown to be at least as good. Moreover, analysis of ordinary least squares models for the monomer melting point clearly showed that such models suffer from over-prediction. The models have been used to predict the properties of two cyanate ester systems that have not yet been synthesized, but could easily be produced for future validation experiments.

Acknowledgement

The authors wish to thank the Strategic Enrivonmental Research and Development Program (project WP-2214), Air Force Office of Scientific Research, the Office of Naval Research, and the Air Force Research Laboratory for their support of these efforts.

References

1. Hamerton, I. In Chemistry and Technology of Cyanate Ester Resins, Hamerton, I., Ed.; Chapman & Hall: London, **1994**; pp 1-6.
2. Fang, T.; Shimp, D. A. *Prog. Polym. Sci.* **1995**, *20*, 61-118.
3. Nair, C. P. R.; Mathew, D.; Ninan, K. N. In *New Polymerization Techniques and Synthetic Methodologies*, Abe, A.; Albertsson, A.-C.; Cantow, H. J., Eds.; Springer-Verlag: Berlin, **2001**; Vol. 155, pp 1-99.
4. Hamerton, I.; Hay, J. N. *High Perform. Polym.* **1998,** *10*, 163-174.
5. Chen, P. C.; Bowers, C. W.; Content, D. A.; Marzouk, M.; Romeo, R. C. *Opt. Eng.* **2000,** *39*, 2320-2329.
6. Wienhold, P. D.; Persons, D. F. *SAMPE J.* **2003,** *39*, 6-17.
7. Shivakumar, K. N.; Chen, H.; Holloway, G. *J. Reinf. Plast. Compos.* **2009**, *28*, 675-689.
8. Fyfe, C. A.; Niu, J.; Rettig, S. J.; Burlinson, N. E.; Reidsema, C. M.; Wang, D. W.; Poliks, M. *Macromolecules* **1992,** *25*, 6289-6301.
9. Davis, M. C.; Guenthner, A. J.; Groshens, T. J.; Reams, J. T.; Mabry, J. M. *J. Polym. Sci. Part A Polym. Chem.* **2012**, *50*, 4127-4136.
10. Meylemans, H. A.; Harvey, B. G.; Reams, J. T.; Guenthner, A. J.; Cambrea, L. R.; Groshens, T. J.; Baldwin, L. C.; Garrison, M. D.; Mabry, J. M. *Biomacromolecules* **2013**, *14*, 771-780.
11. Harvey, B. G.; Guenthner, A. J.; Lai, W. W.; Meylemans, H. A.; Davis, M. C.; Cambrea, L. R.; Reams, J. T.; Lamison, K. R., *Macromolecules*, submitted.
12. Harvey, B. G.; Sahagun, C. M.; Guenthner, A. J.; Groshens, T. J.; Cambrea, L. R.; Reams, J. T.; Mabry J. M. *ChemSusChem*, **2014**, *7*, 1964-1969.
13. Cash, J. J.; Davis, M. C.; Ford, M. D.; Groshens, T. J.; Guenthner, A. J.; Harvey, B. G.; Lamison, K. R.; Mabry, J. M.; Meylemans, H. A.; Reams, J. T.; Sahagun, C. M. *Polym. Chem*. **2013**, *4*, 3859-3865.
14. Guenthner, A. J.; Wright, M. E.; Chafin, A. P.; Reams, J. T.; Lamison, K. R.; Ford, M. D.; Kirby, S. P. J.; Zavala, J. J.; Mabry, J. M. *Macromolecules* **2014**, *47*, 7691-7700.
15. Harvey, B. G.; Guenthner, A. J.; Meylemans, H. A.; Haines, S. R. L.; Lamison, K. R.; Groshens, T. J.; Cambrea, L. R.; Davis, M. C.; Lai, W. W. *Green Chemistry* **2015**, doi 10.1039/C4GC01825G.
16. Bicerano, J., *Prediction of Polymer Properties*. 3rd ed.; Marcel Dekker, Inc.: New York, **2002**; p. 113.
17. de Jong, S. *Chemometr. Intel. Lab.***1993**, *18*, 251–263.
18. Guenthner, A. J.; Reams, J. T.; Lamison, K. R.; Ramirez, S. M.; Swanson, D. D.; Yandek, G. R.; Sahagun, C. M.; Davis, M. C.; Mabry, J. M. *ACS Appl. Mater. Interfaces* **2013**, *5*, 8772-8783.

19. Cambrea, L. R.; Davis, M. C.; Groshens, T. J.; Guenthner, A. J.; Lamison, K. R.; Mabry J. M. *J. Polym. Sci. Part A Polym. Chem.* **2010**, *48,* 4547-4554.